Affinity Labeling and Measurement of DNA-Induced Conformation Change in RNA Polymerase II†

Insug Kang, Johnson Lin, and Jui H. Wang*

Department of Chemistry, Acheson Hall, State University of New York at Buffalo, Buffalo, New York 14214-3094

Received September 24, 1993; Revised Manuscript Received November 15, 1993®

ABSTRACT: The inhibition of RNA polymerase II by 8-azido-2′-*O*-(1-naphthalenesulfonyl)-ATP (AN-ATP) was found to be reversible in the dark and competitive with ATP, with $K_I = 2.2 \pm 0.2$ μM and $K_{ATP} = 20 \pm 0.5$ μM, but noncompetitive with CTP and GTP, with dissociation constants $K_{CTP} = 4.4 \pm 0.4$ μM and $K_{GTP} = 19.4 \pm 0.7$ μM. Under UV irradiation the enzyme was irreversibly labeled by AN-[α-^{32}P]ATP. A linear plot of the relative specific activities of labeled enzyme samples after gel filtration vs the number of labels per enzyme molecule shows that each covalent label completely inactivates an enzyme molecule. Therefore the labeling has maximal specificity at an essential *specific ATP site* which is not the *substrate-binding site* for the polymerization reaction. The fluorescent AN-ATP-labeled enzyme, with absorbance maximum at 310 nm and emission maximum at 370 nm, can still bind noncovalently a second ligand, 2′-*O*-dansyl-ATP, with absorbance maximum at 365 nm and emission maximum at 560 nm, at *the substrate-binding site.* Measurement of energy transfer between the two fluorescent labels gave $R = 23.8 \pm 0.4$ Å as the average distance between them and $K_d = 31 \pm 0.1$ μM for the bound 2′-*O*-dansyl-ATP in the absence of DNA template. The addition of either thymus DNA or poly[d(A-T)] to the system changed these values to $R = 25.6 \pm 0.4$ Å and $K_d = 53 \pm 0.4$ μM. These results indicate that the binding of RNA polymerase II to DNA template triggers a conformation change in the enzyme molecule.

RNA polymerase II has been purified from a variety of eukaryotes and shown to be a multisubunit molecule that can catalyze the nonspecific synthesis of RNA from a DNA template. However, it does not have the ability to initiate programmed transcription accurately and efficiently. In addition to the polymerase itself, a promoter region of the DNA template and seven transcription factors (TFIIs) are required for the initiation process (Maldonado et al., 1990; Buratowski et al., 1990; Sawadogo & Sentenac, 1990; Flores et al., 1991). The catalytic properties of the enzyme are presumably regulated by conformation changes due to specific contact interactions within the enzyme–DNA–TFIIs complex as well as by the catalyzed phosphorylation–dephosphorylation balance in the carboxy-terminal domain of the largest subunit of RNA polymerase II (Cadena & Dahnus, 1987; Payne et al., 1989; Corden, 1990; Laybourn & Dahmus, 1990; Lu et al., 1991, 1992; Flores et al., 1992). For these reasons, information on conformation changes at or near the nucleotide-binding sites of RNA polymerase II may advance our understanding of transcription regulation.

As a first step in the study of function-related conformation change in RNA polymerase II, the effect of enzyme–DNA interaction on protein conformation at or near the nucleoside triphosphate (NTP) binding sites of RNA polymerase II from calf thymus has been examined in this work. The enzyme was first labeled specifically with the fluorescent photoaffinity reagent 8-azido-(1-naphthalenesulfonyl)-[α-^{32}P]ATP (AN-[α-^{32}P]ATP). The covalently labeled enzyme was subsequently labeled noncovalently with 2′-*O*-dansyl-ATP specifically at a second site. Measurement of resonant energy transfer between the two bound fluorescent probes in the absence and presence of DNA shows that the noncovalent contact interaction between DNA and RNA polymerase II induces a protein conformation change in the enzyme.

EXPERIMENTAL PROCEDURES

Purification of RNA Polymerase II. DNA-dependent RNA polymerase II was extracted from fresh calf thymus and purified by the procedure of Hodo and Blatti (1977) as modified by Sopta et al. (1985). The purification involved precipitation with poly(ethylenimine), selective elution of RNA polymerase II from the precipitate, and chromatography of the eluate on DEAE-cellulose (Whatman, DE-52), phosphocellulose (Sigma), and DEAE-Sephadex (Sigma) columns. The enzyme solution was concentrated by reloading onto DEAE-cellulose with 0.1 M KCl and elution of the proteins by 0.6 M KCl. The isolated RNA polymerase II was not significantly contaminated by other nuclear RNA polymerases, because it was totally inhibited by 0.5 μg/mL α-amanitin (Boehringer-Mannheim). Figure 1 shows that the purified RNA polymerase II was found by SDS–PAGE analysis to have the same subunit structure as that reported by Hodo and Blatti, with subunit molecular weights of 210 000, 180 000, 145 000, 44 000, 36 000, 25 000, 20 000, 18 500, 16 000, 15 000, 12 000, and 11 500. The specific activity of the purified RNA polymerase II was 170–200 units/mg, consistent with the value of 160 units/mg of the Hodo and Blatti sample, which was >96% pure.

Enzyme Assay. The reaction solution (50 μL) contained 50 nM enzyme, 20 μg of native thymus DNA templates (Type I, Sigma), 10 μM [α-^{32}P]-UTP (5 μCi) (New England Nuclear), and 200 μM unlabeled nucleotide substrates in buffer A (50 mM Hepes–NaOH, pH 7.9, 10% glycerol, 0.2 mg/mL BSA, 0.5 mM DTT, 0.1 mM EDTA, 5 mM $MgCl_2$, 80 mM $(NH_4)_2SO_4$, and 60 mM KCl). The solutions with all the components except the nucleoside triphosphates were preincubated for 30 min, and then the reactions were initiated by adding nucleotide substrates at 37 °C. After 10 min, the

† This work was supported by Research Grant GM 41610 from the National Institute of General Medical Sciences, National Institutes of Health.

* To whom correspondence should be addressed.

® Abstract published in *Advance ACS Abstracts,* February 15, 1994.

0006-2960/94/0433-2696$04.50/0

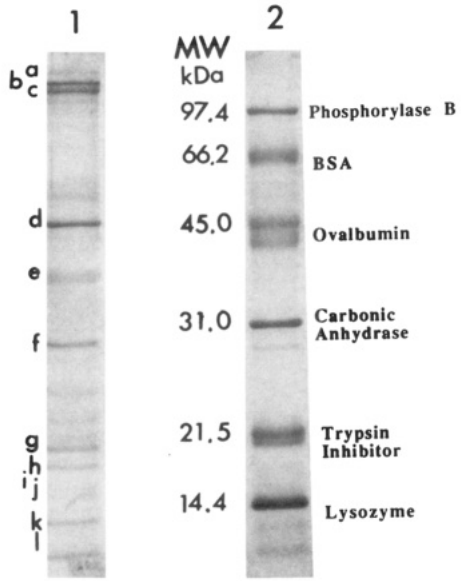

FIGURE 1: Subunit structure of purified calf thymus RNA polymerase II. The purified calf thymus RNA polymerase II eluted sequentially from Sephadex-A25/Bio-Gel A-1.5 m was precipitated by 10% TCA and analyzed on an SDS–12.5% PAGE gel. The molecular weights for the subunits of RNA pol II obtained by comparison with the standards shown on the right are a = 210 000, b = 180 000, c = 145 000, d = 44 000, e = 36 000, f = 25 000, g = 20 000, h = 18 500, i = 16 000, k = 12 000, and l = 11 500.

reactions were terminated by adding 6 mL of 10% TCA and 20 mM sodium pyrophosphate. After another 3 min, the precipitates were collected on Millipore filters (HATF) and each was washed twice with 4 mL of the same TCA solution. Alternatively, aliquots of the reaction mixtures were spotted on GF/C filters (Sigma) as described by Freund and McGuire (1986). The transcription activities were monitored by radioactive counting of the dried filters. Both methods gave the same results. Protein concentrations were determined by the Coomassie Blue binding method (Bradford, 1976). RNA polymerase activity was measured in units. One unit is defined as the amount of RNA polymerase that catalyzes the incorporation of 1 pmol of UMP into RNA in 10 min under the above described conditions.

Synthesis of 8-Azido-2′-O-(1-naphthalenesulfonyl)-ATP. AN-ATP was synthesized by essentially the same procedure as that used previously for 8-azido-2′-*O*-dansyl-ATP (AD-ATP) (Chuan et al., 1989). In a typical experiment, 5 mg of 8-azido-ATP (Sigma) or 8-azido-[α-^{32}P]ATP (ICN) was dissolved in 0.1 mL of 0.3 M K_2CO_3/0.65 M $KHCO_3$ buffer at pH 9.6 in the dark. A solution of 7.7 mg of 1-naphthalenesulfonyl chloride (Aldrich) in 0.4 mL of acetone at 0 °C was prepared and added in three aliquots at 1-h intervals to the above 8-azido-ATP solution in the dark with stirring at 0–4 °C. After 2 h, the reaction was allowed to continue at 28 °C for 18 h until 1-naphthalenesulfonyl chloride was no longer detectable by TLC analysis (using 8-azido-ATP and ethyl 1-naphthalenesulfonate as model compounds). The cloudy mixture was then separated on TLC (Baker Si-250) with a solvent mixture of 1-propanol/1.0 M ammonium acetate (2:1). The AN-ATP band (R_f = 0.54) was scraped off and extracted with water. The extract was lyophilized and assayed. The yield was 40–50%. Measurements of absorbance at 259 and 310 nm, respectively, gave an adenine to naphthalenesulfonyl group molar ratio of 1:1. A 2-mg sample of this purified product was dissolved in D_2O, adjusted to pH 6.5–7.0 with NaOD in D_2O solution, and again lyophilized and redissolved three times to replace all the exchangeable ^{1}H by ^{2}H for NMR measurement. A comparison of the ^{1}H NMR spectrum of AN-ATP with that of ATP (Chuan et al., 1989) indicated that the naphthalenesulfonyl group is attached to the 2′-*O*-position of ribose.

Synthesis of 2′-O-Dansyl-ATP. Ten milligrams of ATP was dissolved in 0.2 mL of 0.3 M K_2CO_3/0.85 M $KHCO_3$ buffer, pH 9.6. The reaction was started by the addition of three aliquots of 15 mg of dansyl chloride in 0.8 mL of acetone solution at 0 °C at 1-h intervals and subsequently allowed to react at 28 °C another 16 h. The mixture was then separated on TLC with the 1-propanol/1.0 M ammonium acetate (2:1) solvent mixture. The DNS-ATP band (R_f = 0.48) on TLC was scraped off and extracted with water. The extract was lyophilized and assayed.

Inhibition of RNA Polymerase II by AN-ATP in the Dark. The enzyme assays were performed as described above, except that the reaction solutions containing RNA polymerase II and native calf thymus DNA were preincubated with different concentrations of AN-ATP and ATP in the dark for 30 min before the assay reaction. For reversible competitive inhibition experiments, different concentrations of one nucleotide substrate were introduced into the assay solutions in the presence of different concentrations of AN-ATP in the dark prior to initiation of the transcription assay, while the concentrations of the other substrates were kept constant. The range of concentrations of the variable substrate and that of AN-ATP for each inhibition was chosen near the K_m and K_I values.

Photoaffinity Labeling of RNA Polymerase II by AN-ATP and AD-ATP. A solution containing 1.8 μM RNA polymerase II and 54 μM AN-[α-^{32}P]ATP was incubated in the dark for 30 min and subsequently irradiated by UV light. In order to slow down the photoreaction to a rate convenient for monitoring, a long-wavelength UV lamp with maximum intensity at 365 nm (350 μW at 6 in.) was used so that only its small short-wavelength tail was utilized to activate the AN-ATP. Aliquots were removed from the reaction mixture at proper time intervals and assayed for enzyme activity, protein concentration, and radioactivity after centrifugal gel filtration through Sephadex G-50–80 to separate the native and modified enzyme from the free and noncovalently bound An-[α-^{32}P]ATP. The photoaffinity labeling of RNA polymerase II by AD-ATP was conducted in a similar way but using AD-[α-^{32}P]ATP instead of AN-[α-^{32}P]ATP.

Fluorescence Measurements. The fluorescence emission of AN-ATP-labeled RNA polymerase II under 310-nm exciting light was measured with a Hitachi–Perkin-Elmer fluorescence spectrophotometer (MPF-2A). Calibration measurements show that, after correction for Raman scattering by the medium, the intensity of fluorescence was proportional to the concentration of AN-ATP-labeled RNA polymerase II. A 0.2-mL sample of AN-ATP-labeled RNA polymerase II solution in buffer A was placed in a 0.2-cm diameter cylindrical microfluorescence quartz cell for each measurement. Aliquots (1- or 2-μL) of a stock solution of 2′-*O*-dansyl-ATP (DNS-ATP) was added successively with glass micropipettes (with rinsing) in energy transfer studies.

In order to obtain the fluorescence due to AN-ATP-labeled RNA polymerase II, the observed fluorescence of the solution should be corrected for the weak fluorescence due to free and bound DNS-ATP in the solution. A reference solution containing 3.51 μM unlabeled RNA polymerase II in buffer A was titrated by the successive addition of 1- or 2-μL aliquots of DNA-ATP solution in exactly the same way as the AN-ATP-labeled RNA polymerase II sample solution. For each total DNS-ATP concentrations, the observed fluorescence

emission by AN-ATP-labeled RNA polymerase II was obtained as the difference in fluorescence between the sample and the reference solutions. The DNS-ATP was prepared by reacting ATP with dansyl chloride purified by TLC and identified by ^1H NMR as in the preparation of 8-azido-2′-*O*-dansyl-ATP (AD-ATP) (Chuan et al., 1989).

Since the exciting light at 310 nm and the emitted light monitored at 370 nm were both attenuated by increasing concentrations of DNS-ATP, each observed fluorescence intensity was multiplied by an appropriate factor to correct for this inner filter effect. For the sample in a 0.2-cm diameter cylindrical cell, the exciting light is attenuated approximately by a factor of $10^{-A_{310}/10}$ and the emitted light is attenuated approximately by a factor of $10^{-A_{370}/10}$. Consequently, each observed fluorescence intensity was multiplied by an overall correction factor of $10^{\langle A \rangle}$ due to the inner filter effect, where $\langle A \rangle = (A_{310} + A_{370})/10$.

The quantum efficiency of AN-ATP-labeled RNA polymerase II (AN-ATP-pol II) was found to be 15.0% by using quinine sulfate with a quantum efficiency (Q_{qs}) of 0.70 ± 0.02 as the reference standard according to

$$Q_{\text{AN-ATP-pol II}} = Q_{qs}(I_{320}/I_{310})(f_{\text{AN-ATP-pol II}}/f_{qs})(A_{qs}/A_{\text{AN-ATP-pol II}})$$

The ratio I_{320}/I_{310} of the intensities of the xenon light source at 320 and 310 nm, respectively, was found to be 1.36. The ratio of total emission output f of 1.6 μM (n = 0.59) AN-ATP-labeled RNA polymerase II solution to that of 50 nM quinine sulfate in 0.1 N H_2SO_4 solution was found to be 2.37 by graphical integration. The ratio $A_{qs}/A_{\text{AN-ATP-pol II}}$ of the absorbance of the quinine sulfate solution at 320 nm to that of the AN-ATP-labeled RNA polymerase II at 310 nm was computed from the measured values obtained at higher concentrations and was found to be 0.067.

RESULTS

Reversible Inhibition in the Dark. The inhibition of transcription activity of RNA polymerase II (50 nM) by AN-ATP in the dark was investigated with calf thymus DNA template and [α-^{32}P]UTP. Figure 2 shows that the concentration of AN-ATP that is required for 50% inhibition of enzyme activity is 2.3 ± 0.4 μM, indicating that AN-ATP is a good inhibitor for RNA polymerase II.

The inset of Figure 2 shows that this inhibition in the dark is reversible and competitive between AN-ATP and ATP, with an inhibition constant of K_I = 2.2 ± 0.2 μM for AN-ATP and K_{ATP} of 20 ± 0.5 μM for ATP, according to

$$\frac{1}{V} = \frac{1}{V_{max}}\left[1 + \frac{K_{ATP}}{[ATP]}\left(1 + \frac{[I]}{K_I}\right)\right]$$

Thus AN-ATP is bound to this specific ATP site of calf thymus RNA pol II with a 9-fold higher affinity than ATP itself. This K_I value is also 200-fold lower than that of 8-azido-ATP (0.4 mM) (Freund & McGuire, 1986), which explains why AN-ATP is a much more specific photolabeling reagent than 8-azido-ATP.

On the other hand, panels A and B of Figure 3 show that the reversible inhibition of RNA pol II by AN-ATP in the dark is noncompetitive with CTP and GTP, respectively. In reversible noncompetitive inhibition the V_{max} in the above equation is changed to $(V_{max})_i$ by a factor of

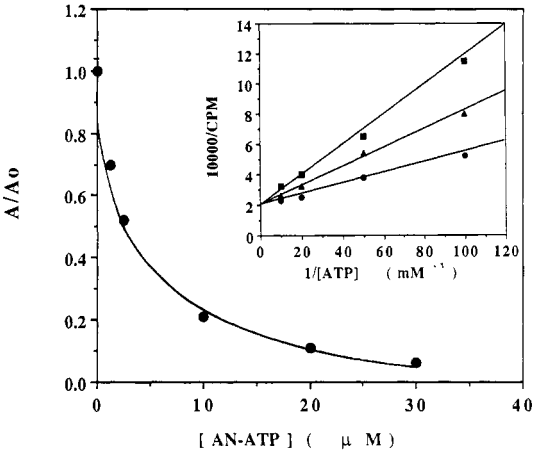

FIGURE 2: Inhibition of calf thymus RNA polymerase II in the dark by different concentrations of AN-ATP. The reaction mixtures (50 μL) containing 50 nM calf thymus RNA polymerase II and 20 μg of native thymus DNA were mixed with increasing concentrations of AN-ATP. The enzyme activity was measured as described under Experimental Procedures. The IC_{50} value was determined by nonlinear regression computer analysis based on the approximate equation % inhibition = 100[I]/(IC_{50} + [I]), where [I] was concentration of AN-ATP. Inset: Competitive inhibition of calf thymus RNA polymerase II in the dark by AN-ATP. Each reaction mixture (50 μL) contained 50 nM calf thymus RNA polymerase II and 20 μg of calf thymus DNA. The ATP concentrations used are indicated in the figure. The final concentrations of AN-ATP were 0 (●), 1.80 μM (▲), and 4.0 μM (■). In the inset, 4350 cpm is equal to 15.8 pmol of UMP incorporated in 1 min at 37 °C/mg of protein, and the reaction velocity can be readily translated to picomoles per milligram per minute.

$$\frac{(V_{max})_i}{V_{max}} = \frac{K_{NTP}}{[I] + K_{NTP}}$$

where K_{NTP} denotes the dissociation constant of the bound substrate. Computation from the data gave K_{CTP} = 4.4 ± 0.4 μM and K_{GTP} = 19.4 ± 0.7 μM.

Photoaffinity Labeling of the Specific ATP Site. In order to investigate the correlation between the extent of covalent labeling of the enzyme by AN-ATP under UV light and the inhibition, both AN-[α-^{32}P]ATP and AD-[α^{32}P]ATP were used as the photoaffinity labeling reagents. A solution containing 1.8 μM RNA polymerase II and 54 μM of radioactive AN-ATP was irradiated under long-wavelength UV light. Aliquots were removed and assayed for enzyme activity, protein concentration, and radioactivity immediately after centrifugal gel filtration through Sephadex G-50–80.

Figure 4A shows the time course of photoinactivation. Upon irradiation, a photoreactive nitrene intermediate was formed which subsequently inactivated the RNA polymerase II. The ratio r of the specific activity of the labeled enzyme to that of the unlabeled control decreased from 1 to 0 after 20 min of irradiation. The control enzyme that was irradiated without AN-ATP did not lose any transcriptional activity. The inset shows that the photolabeling obeys first-order kinetics with a half-time of $t_{1/2}$ = 3.5 min, which corresponds to a pseudo-first-order rate constant of $k' = -d(\ln r)/dt$ = 0.24 min^{-1}.

Figure 4B shows that the observed value of r decreased linearly from 1 to 0 as the number n of the labels incorporated per RNA polymerase II molecule increased from 0 to 1. The linear r versus n plot shows that 1 radioactive label/polymerase molecule is sufficient for complete inactivation of the enzyme. Thus, under the reaction conditions, RNA polymerase II was photolabeled by AN-[α-^{32}P]ATP with maximum specificity, i.e., no nonspecific covalent labeling.

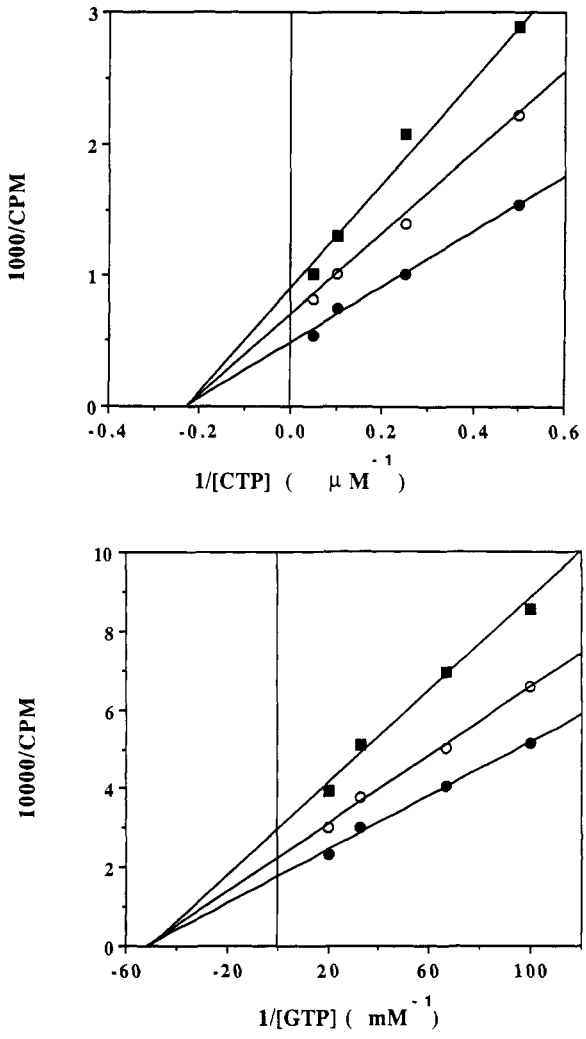

FIGURE 3: (A, top) Noncompetitive inhibition of calf thymus RNA polymerase II between AN-ATP and CTP. Each reaction mixture (50 μL) contained 50 nM calf thymus RNA polymerase II and 20 μg of calf thymus DNA. The ATP concentrations used are indicated in the figure. The final concentrations of AN-ATP were 0 (●), 1.60 μM (○), and 3.60 μM (■). In this experiment, 1820 cpm can be converted to 15.4 pmol of UMP incorporated in 1 min at 37 °C/mg of protein, and the reaction velocity can be readily translated to picomoles per milligram per minute. (B, bottom) Noncompetitive inhibition of calf thymus RNA polymerase II between AN-ATP and GTP. Each reaction mixture (50 μL) contained 50 nM calf thymus RNA polymerase II and 20 μg of calf thymus DNA. The ATP concentrations used are indicated in the figure. The final concentrations of AN-ATP were 0 (○), 1.20 μM (●), and 3.0 μM (■). In this experiment, 4310 cpm is equal to 16.4 pmol of UMP incorporated in 1 min at 37 °C/mg of protein, and the reaction velocity can be readily translated to picomoles per milligram per minute.

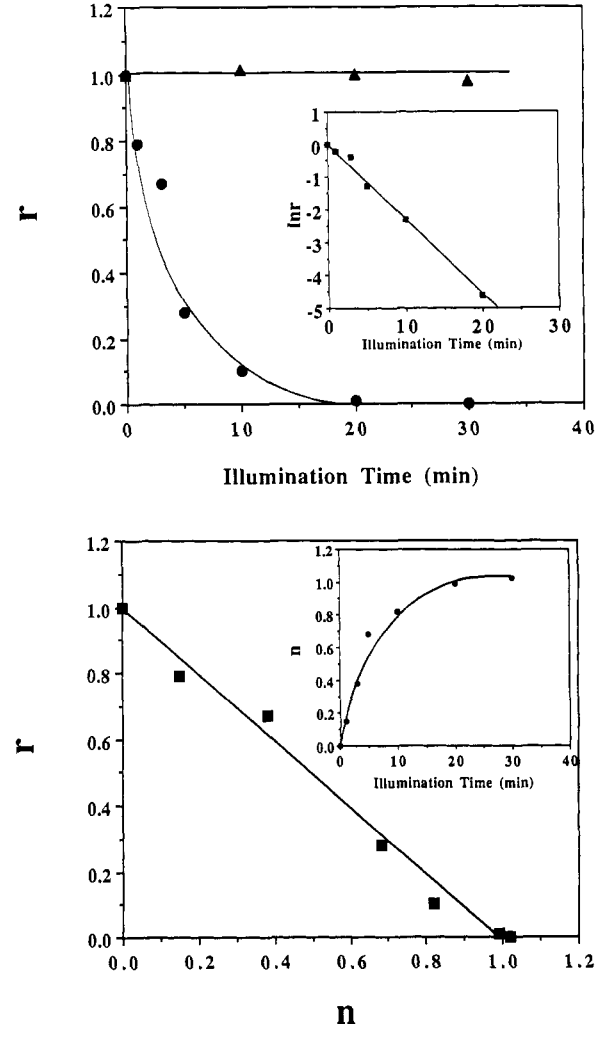

FIGURE 4: (A, top) Time course of photoaffinity labeling of calf thymus RNA polymerase II by AN-ATP. A solution of 1.8 μM RNA polymerase II with 54 μM AN-[α-^{32}P]ATP was irradiated under 365-nm UV light. Equal-amount aliquots were removed from the reaction mixture at 1-, 3-, 5-, 10-, 20-, and 30-min intervals and gel-filtered through Sephadex G-50–80. The enzyme activity, protein concentration, and radioactivity were assayed right after gel filtration. *n* represents the molar ratio of AN-ATP-label to RNA polymerase II. *r* denotes the ratio of the transcription specific activity of labeled enzyme to that of the controlled one under standard conditions as described under Experimental Procedures. Inset: Plot with ordinate as a logarithmic scale. (B, bottom) Correlation between the covalent binding of AN-ATP label and the catalytic activity of RNA pol II. The linear plot with slope $dr/dn = -1$ shows that 1 radioactive label/RNA polymerase II molecule is sufficient for complete inactivation of the enzyme. Inset: Time course of photoaffinity labeling.

In order for RNA pol II to function, its *substrate-binding site* should be able to bind any one of the four nucleotide triphosphates. Since the site that can be labeled specifically by AN-ATP does not bind CTP or GTP (Figure 3), it cannot be the *substrate-binding site*. But since this *specific ATP site* is essential for the initiation of transcription, it could be the specific site where the required ATP hydrolysis takes place prior to RNA synthesis. Previous studies showed that ATP hydrolysis is necessary for activating transcription initiation (Bunick et al., 1982; Savadogo & Roeder, 1984; Rappaport & Weinstein, 1987; Conaway & Conaway, 1988) and that RNA synthesis was inhibited when ATP was replaced by 5′-adenylyl imidodiphosphate (AMP-PNP), which could block the energy-requiring step that leads to melting and transcription of the double-stranded DNA template (Cat & Luse, 1987; Wang et al., 1992). Inasmuch as 8-azido-ATP cannot be used as a substrate for RNA pol II even in the dark (Freund & McGuire, 1986), it is probably not bound to the *substrate-binding site* but could still be bound at the *specific ATP site* and act as an inhibitor competitive with ATP. The reversible inhibition of RNA pol II by AN-ATP in the dark could be explained similarly if we assume that because of stereochemical reasons all 8-azido derivatives of ATP could be bound only at the *specific ATP site* (Figure 4B) but not at the *substrate-binding site*. Then its inhibition in the dark should also be competitive with ATP, which can be bound at both sites, but noncompetitive with CTP or GTP, which can be bound only at the *substrate-binding site*.

The *substrate-binding sites* of RNA polymerases I, II, and III from yeast were labeled with the 4-formylphenyl γ-ester of ATP as priming nucleotide followed by reduction with

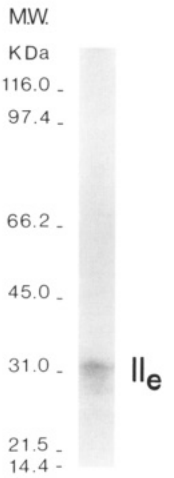

FIGURE 5: Autoradiogram of SDS–10% PAGE showing photoaffinity labeling of calf thymus polymerase II by AD-[α-^{32}P]ATP. The gel was stained and destained, followed by autoradiography of the dried gel. Of the 11 identified polypeptides of the polymerase in Figure 1, only one polypeptide of $M_r \approx 34$ kDa was found to be labeled by radioactive AD-ATP. The three or four additional negative charges on the AD-ATP label could have caused the labeled subunit in Figure 5 to move faster in the electric field than the corresponding unlabeled subunit in Figure 1.

$NaBH_4$. After subsequent phosphodiester formation with [α-^{32}P]UTP, only the second largest subunit of each enzyme (135, 150, and 128 kDa, respectively) was covalently labeled in a template-dependent reaction (Riva et al., 1987). The *specific ATP site* in RNA pol II from calf thymus was also photolabeled with 8-azido-[α-^{32}P]ATP by Freund and McGuire (1986), who found that the covalent label was attached to a smaller subunit of about 37 000 molecular weight. In the present work, calf thymus RNA polymerase II was photolabeled with either AN-[α-^{32}P]ATP or 8-azido-2′-*O*-dansyl-[α-^{32}P]ATP. We found that the latter radioactive label was also covalently attached to a much smaller subunit of about 34 000 molecular weight as shown by the autoradiogram in Figure 5.

Quenching of the Fluorescence of the AN-ATP-Labeled RNA Pol II by 2′-O-Dansyl-ATP. DNS-ATP inhibits RNA pol II with an IC_{50} of about 30 μM. It can presumably be bound to both the *specific ATP site* and the *substrate-binding site* of the enzyme. Since DNS-ATP can only be bound noncovalently to the *substrate-binding site* of RNA pol II, whereas AD-ATP cannot be bound to this site at all, it is not possible to label the *substrate-binding site* of RNA pol II covalently with either of these two reagents. On the other hand, when increasing amounts of DNS-ATP were added to a solution of AN-ATP-labeled RNA pol II, the fluorescence at 370 nm (after small corrections due to the inner filter effect) continued to decrease (curve B, Figure 6). Since the addition of ATP to the labeled enzyme did not cause a similar decrease in the fluorescence (curve A, Figure 6), we may conclude that this observed decrease in fluorescence is not due to ligand-induced protein conformation change but probably due to resonant energy transfer from the covalently bound AN-ATP label (absorbance maximum at 310 nm, emission maximum at 370 nm) to the noncovalently bound DNS-ATP (absorbance maximum at 365 nm, emission maximum at 560 nm). The large overlap of the emission spectrum of the AN-ATP-labeled enzyme and the absorption spectrum of DNS-ATP shown in Figure 7 suggest that resonant energy transfer from the former to the latter can be quite efficient. With 310-nm excitation, the fluorescence of unlabeled RNA pol II was negligible and the very weak fluorescence due to DNS-ATP at 370 nm was

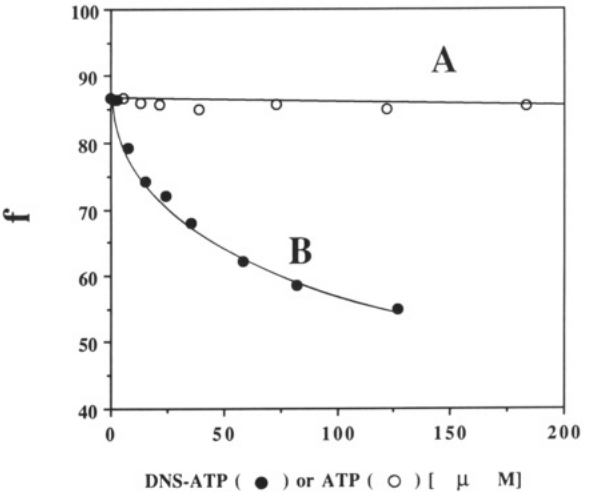

FIGURE 6: Effect of binding ATP or DNS-ATP at the second binding site (substrate-binding site) of AN-ATP-labeled RNA pol II on its fluorescence at 370 nm.

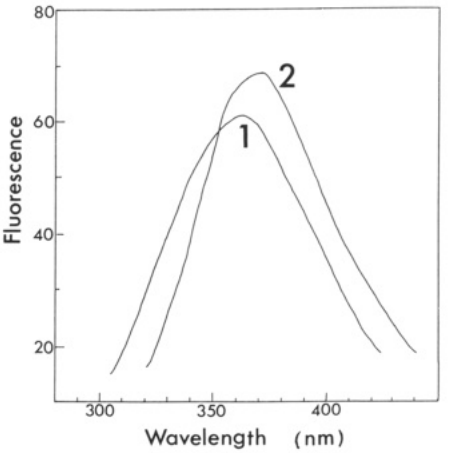

FIGURE 7: Spectral overlap for efficient energy transfer from AN-ATP-labeled RNA polymerase II to DNS-ATP. Curve 1, absorption spectrum of DNS-ATP. Curve 2, emission spectrum of AN-ATP-labeled RNA polymerase II with excitation at 310 nm.

substracted from all measured values.

The overlap integral in Föster's theory of the energy transfer is

$$J = [\int_0^\infty f_D(\nu)\epsilon_A(\nu)\ (d\nu/\nu^4)]/[\int_0^\infty f_D(\nu)\ (d\nu/\nu^4)]$$

where the subscripts D and A refer to donor and acceptor groups, respectively, was computed by the approximate equation that was used by Cantley and Hammes (1975):

$$J = \sum_\lambda f_D(\lambda)\epsilon_A(\lambda)\lambda^4\ \Delta\lambda / \sum_\lambda f_D(\lambda)\ \Delta\lambda$$

by choosing $\Delta\lambda = 5$ nm and summing over the entire emission spectrum of AN-ATP-labeled RNA polymerase II in buffer A (Figure 7), it was found that $J = 6.75 \times 10^{-15}$ cm^6/mmol.

In order to obtain the fluorescence due to AN-ATP-labeled RNA polymerase II, the observed fluorescence (f) of the solution was corrected for the very weak fluorescence due to free and bound DNS-ATP in the solution. A reference solution containing 3.51 μM labeled RNA polymerase II in buffer A was titrated by the successive addition of 1- or 2-μL aliquots of DNS-ATP solution in exactly the same way as the AN-ATP-labeled RNA polymerase II sample solution was titrated. For each total DNS-ATP concentration, the observed fluo-

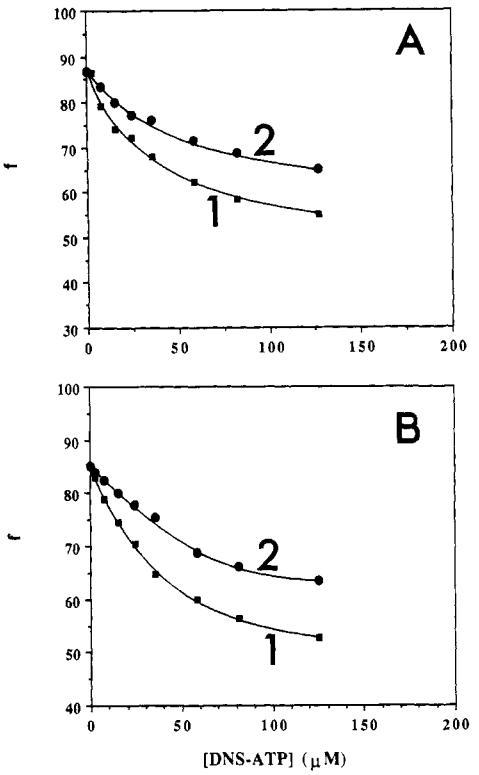

FIGURE 8: (A) Quenching of the fluorescence of AN-ATP-labeled RNA polymerase II by DNS-ATP in the absence or presence of calf thymus DNA. All samples were in 0.2 mL of buffer (50 mM Hepes–NaOH, pH 7.9, 20% glycerol, and 2 mM EDTA). Excitation was at 310 nm, and the emission intensities at 370 nm were recorded. Curve 1, 3.51 μM RNA polymerase II (n = 0.89) + DNS-ATP. The excitation and emission band widths were 4.5 and 6.5 nm, respectively. f_1 = 86.7, f_2 = 47.0. Curve 2, 3.51 μM RNA polymerase II (n = 0.89) in buffer A + 200 μg of calf thymus DNA. f_1 = 86.7 f_2 = 56.0. (B) Quenching of the fluorescence of AN-ATP-labeled RNA polymerase II by DNS-ATP in the absence or presence of poly[d(A-T)]. All samples were in 0.2 mL of buffer. Curve 1, 2.20 μM RNA polymerase II (n = 0.89) + DNS-ATP. The excitation and emission band widths were 5.5 and 7.5 nm, respectively. f_1 = 84.5, f_2 = 45.0. Curve 2, 2.20 μM RNA polymerase II (n = 0.89) in buffer A + 200 μg of poly[d(A-T)]. f_1 = 84.5, f_2 = 54.0.

rescence emission by AN-ATP-labeled RNA polymerase II was obtained as the difference in fluorescence between the sample and reference solutions.

The corrected fluorescence of AN-ATP-labeled enzyme was measured as a function of DNS-ATP concentration both in the absence and in the presence of DNA templates. The results are summarized in Figure 8.

Template-Induced Change in Protein Conformation. The effect of template binding on the fluorescence of the AN-ATP-labeled enzyme in the presence of DNS-ATP as shown in Figure 8 is quite conspicuous. Even without further treatment, these results can already lead us to certain conclusions: (A) In the absence of DNS-ATP, the binding of template to AN-ATP-labeled RNA pol II does not affect the fluorescence of the labeled enzyme. This implies either that there is no conformation change at the active site or that the conformation change did not alter the dielectric environment of the AN-ATP label. (B) In the presence of 10–150 μM DNS-ATP, the binding of template to AN-ATP-labeled RNA pol II enhances the fluorescence of the labeled enzyme. The enhancement increases with DNS-ATP concentration. This observation indicates that there is template-induced conformation change which increases either the average distance between the two bound labels or the K_d of the noncovalently bound label or both and thereby lowers the efficiency of energy transfer process. (C) The binding of calf thymus DNA or poly[d(A-T)] to the AN-ATP-labeled enzyme leads to similar fluorescence enhancement in DNS-ATP solutions. This observation suggests that by itself RNA pol II does not bind template molecules discriminatively, which is consistent with its ability to catalyze nonspecific synthesis of RNA from a DNA template in the absence of transcription factors.

DISCUSSION

The data in Figure 8 can be treated quantitatively to obtain more detailed information. Let us represent the dissociation equilibrium for the DNS-ATP bound at the substrate-binding site of AN-ATP-labeled RNA pol II (E) by

$$\text{E-DNS-ATP} \overset{K_d}{\rightleftarrows} \text{E} + \text{DNS-ATP}$$

where

$$K_d = [(a-x)(b-x)]/x \quad (1)$$

a and b represent the total molar concentrations of the labeled enzyme and DNS-ATP, respectively, and x = [E-DNS-ATP].

The observed fluorescence intensity f is given by

$$af = (a-x)f_2 + xf_1 \quad (2)$$

where f_1 and f_2 represent the fluorescence intensities of E and E-DNS-ATP, respectively. Combining eqs 1 and 2, we obtain

$$\frac{f_1-f}{f-f_2} = \left(\frac{1}{K_d}\right)\left[b - \frac{a(f_1-f)}{f_1-f_2}\right] \quad (3)$$

In each experiment f_1 and various values of f were measured directly. f_2 was determined iteratively as a parameter that gives the best-fitting linear $(f_1-f)/(f-f_2)$ vs $b-[a(f_1-f)/(f_1-f_2)]$ plot. The slope of linear plot is equal to $1/K_d$. The data from two matching pairs of experiments, with calf thymus DNA and poly[d(A-T)] (Sigma), respectively, as the template, are plotted in this way in Figure 9.

The efficiency of energy transfer E from the AN-ATP label to the bound DNS-ATP is given by

$$E = (R_{1/2}/R)^6/[(R_{1/2}/R)^6 + 1] \quad (4)$$

or

$$R = R_{1/2}[(1-E)/E]^{1/6} \quad (5)$$

where R is the distance between the donor and acceptor groups (Föster, 1948; Stryer & Haughland, 1967). $R_{1/2}$ is the distance corresponding to 50% transfer efficiency and is given by

$$R_{1/2} = (9.79 \times 10^3)(\kappa^2 Q J n^{-4})^{1/2} \quad (6)$$

where κ is the relative orientation factor of the oscillating dipoles, Q is the quantum yield of AN-ATP label in the absence of DNS-AT, J is the overlap integral, and n is the refractive index of the medium.

For the present system, the overlap integral has already been computed from Figure 7 to be $J = 6.75 \times 10^{-15}$ cm^6/mmol and Q is equal to 0.15. By choosing $\kappa^2 = {}^2/_3$ (the average value for random orientation) and n = 1.4, we obtain from eq 6 the value $R_{1/2}$ = 23.2 Å. Since the experimentally determined energy transfer efficiency is given by $E = (f_1 - f_2)/f_1$, the actual distance R is readily computed from eq 5. The calculated results of duplicate experiments are summa-

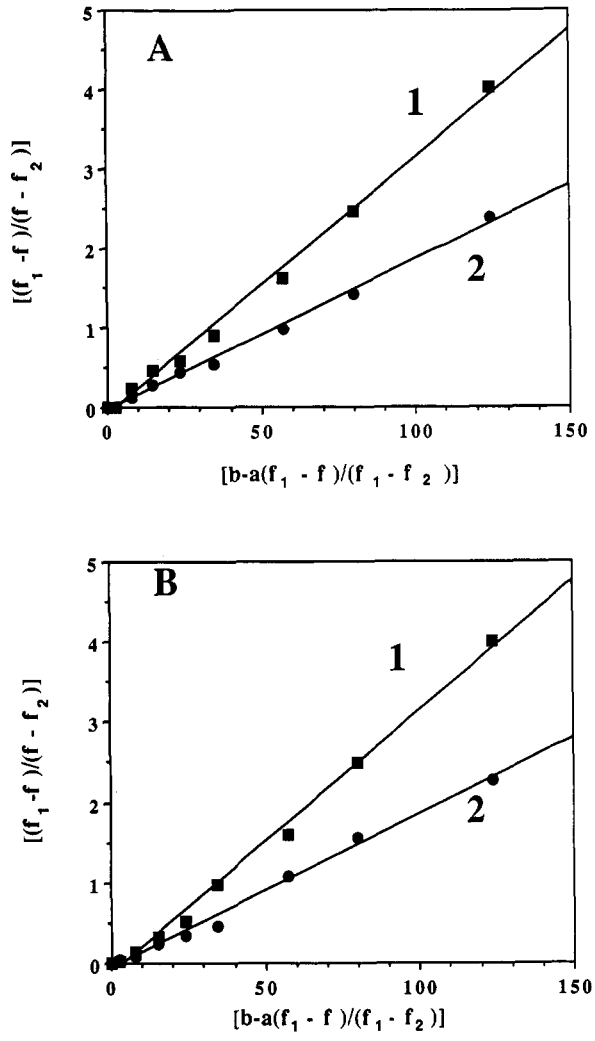

FIGURE 9: Verification of eq 3 and determination of R and K_d from the quenching of fluorescence of AN-ATP-labeled RNA pol II by DNS-ATP. (A) Curve 1, no template; curve 2, with the addition of thymus DNA. (B) Curve 1, no template; curve 2, with the addition of poly[d(A-T)]. The concentrations are given in the caption of Figure 8.

rized below, where E denotes the AN-ATP-labeled RNA pol II. Because R is proportional to $[(1-E)/E]^{1/6}$, the uncertainty in its calculated value is only ±0.4 Å.

E + DNS-ATP	R = 23.9 Å	K_d = 31 μM
E + thymus DNA + DNS-ATP	R = 25.7 Å	K_d = 53 μM
E + DNS-ATP	R = 23.7 Å	K_d = 31 μM
E + poly[d(A-T)] + DNS-ATP	R = 25.5 Å	K_d = 53 μM

These results show that the binding of DNA template to the doubly labeled RNA pol II induces a conformation change in the enzyme which increases the average distance between the two affinity labels bound at specific nucleotide binding sites. The binding also increases the K_d of the noncovalently bound label. There is the possibility that conformation change in RNA pol II due to either catalyzed phosphorylation of the carboxy-terminal domain of its largest subunit or interaction between transcription factors and the enzyme–DNA complex can be monitored in a similar way.

REFERENCES

Bradford, M. M. (1976) *Anal. Biochem. 72*, 248–254.

Bunick, D., Zandomeni, R., Ackerman, S., & Weinmann, R. (1982) *Cell 29*, 877–886.

Buratowski, S., Hahn, S., Fuarente, L., & Sharp, P. A. (1990) *Cell 56*, 549–561.

Cadena, D., & Dahmus, M. (1987) *J. Biol. Chem. 262*, 12468–12474.

Cantley, L. C., & Hammes, G. G. (1975) *Biochemistry 14*, 2976–2981.

Cat, H., & Luse, D. S. (1987) *Mol. Cell. Biol. 7*, 337.

Chuan, H., Lin, J., & Wang, J. H. (1989) *J. Biol. Chem. 264*, 7981–7988; correction (1990) *J. Biol. Chem. 265*, 594.

Conaway, R. C., & Conaway, J. W. (1988) *J. Biol. Chem. 263*, 2962–2968.

Corden, J. F. (1990) *Trends Biochem. Sci. 15*, 383–387.

Flores, O., Lu, H., Killeen, M., Greenblatt, J., & Reinberg, D. (1991) *Proc. Natl. Acad. Sci. U.S.A. 88*, 9999–10003.

Flores, O., Lu, H., & Reinberg, D. (1992) *J. Biol. Chem. 267*, 2786–2793.

Föster, T. (1948) *Ann. Phys. (Leipzig) 2*, 55–75.

Freund, E., & McGuire, P. M. (1986) *Biochemistry 25*, 276–284.

Hodo, H. G., & Blatti, S. P. (1977) *Biochemistry 16*, 2334–2343.

Laybourn, P. J., & Dahmus, M. (1990) *J. Biol. Chem. 265*, 13165–13173.

Lin, J. (1992) Ph.D. Dissertation, Department of Chemistry, State University of New York at Buffalo.

Lu, H., Flores, O., Weinmann, R., & Reinberg, D. (1991) *Proc. Natl. Acad. Sci. U.S.A. 88*, 10004–10008.

Lu, H., Zawel, L., Fisher, L., Egly, J.-M., & Reinberg, D. (1992) *Nature 358*, 641–645.

Maldonado, E., Ha, I., Cortes, P., Weis, L., & Reinberg, D. (1990) *Mol. Cell. Biol. 10*, 6335–6347.

Payne, J. M., Laybourn, P. J., & Dahmus, M. (1989) *J. Biol. Chem. 264*, 19621–19629.

Rappaport, J., & Weinmann, R. (1987) *J. Biol. Chem. 262*, 17510–17515.

Riva, M., Schaffner, H. R., Sentenac, A., Hartman, G. R., Mustaev, A. A., et al. (1987) *J. Biol. Chem. 262*, 14377–14380.

Sawadogo, M., & Roeder, R. G. (1984) *J. Biol. Chem. 258*, 5321–5326.

Sawadogo, M., & Sentenac, A. (1990) *Annu. Rev. Biochem. 59*, 711–754.

Sopta, M., Carthew, R. W., & Greenblatt, J. (1985) *J. Biol. Chem. 260*, 10353–10360.

Stryer, L., and Haughland, R. P. (1967) *Proc. Natl. Acad. Sci. U.S.A. 58*, 719–726.

Wang, W., Carey, M., & Gralla, J. D. (1992) *Science 255*, 450–453.

Wu, J. C., & Wang, J. H. (1989) *J. Biol. Chem. 264*, 9989–9993.